Characterization of the Metal Phase in NM/$Ce_{0.68}Zr_{0.32}O_2$ (NM: Pt and Pd) Catalysts by Hydrogen Chemisorption and HRTEM Microscopy: A Comparative Study

José M. Gatica,[†,‡] Richard T. Baker,[‡,§] Paolo Fornasiero,[†] Serafín Bernal,[‡] and Jan Kašpar*[,†]

Dipartimento di Scienze Chimiche, Università di Trieste, Via Giorgieri 1, I-34127 Trieste, Italy, and Departamento de Ciencia de los Materiales e Ingeniería Metalúrgica y Química Inorgánica, Universidad de Cádiz, E-11510 Puerto Real (Cadiz), Spain

Received: October 4, 2000; In Final Form: December 1, 2000

Pt and Pd particles supported on a texturally stable $Ce_{0.68}Zr_{0.32}O_2$ mixed oxide were investigated by means of H_2 chemisorption and high-resolution transmission electron microscopy (HRTEM). The comparison of the metal dispersion data as determined by HRTEM with those estimated from H_2 volumetric adsorption reveals that, in the case of Pt catalysts reduced at temperatures below 350 °C, the chemisorption isotherms recorded at −80 °C provide reliable dispersion data. For catalysts reduced at, or above, 350 °C, some platinum deactivation occurred. However, H_2 chemisorption capability was recovered by reoxidation at 427 °C and further reduction at 150 °C. For catalysts reduced at 700 °C or 900 °C, the recovery of the platinum chemisorptive capability was only partial, even if a more severe reoxidation treatment (700 °C) was applied. To prevent hydride formation, H_2 chemisorption on the Pd/$Ce_{0.68}Zr_{0.32}O_2$ was investigated at low H_2 pressures and at room temperature. Under these experimental conditions, which are often employed for characterizing Pd catalysts, hydrogen spillover cannot be blocked, thus preventing a reliable estimate of the metal dispersion in our ceria−zirconia -supported palladium catalysts.

1. Introduction

Characterization of noble metal (NM)-containing CeO_2−ZrO_2 mixed oxides represents a challenge both from the fundamental and the industrial point of view. In fact these materials are extensively employed in modern automotive three-way catalysts, as well as in industrial catalysis.[1]

Studies of the interaction of small molecules such as H_2, CO, NO, and O_2 with these materials have also revealed unusual properties. In particular, they have shown themselves to be highly efficient at releasing, activating, and acquiring oxygen, which makes these materials very effective oxidation/reduction catalysts.[1−6] This key property has been attributed to the highly labile Ce^{4+}/Ce^{3+} redox couple in the ceria−zirconia mixed oxide lattice. In the presence of highly dispersed NMs, this redox activity starts at temperatures as low as 170 °C.[7]

The interaction of H_2 with NM/CeO_2-based materials is particularly intriguing since both H_2 adsorption on the metal and extensive spillover of H-species onto the support are detected even at room temperature.[8] In addition to its essential role in determining the redox behavior of these systems, spillover of H atoms has a relevant influence on the catalytic behavior of CeO_2- and ZrO_2-containing materials. Such is the case in the partial oxidation of methane over Pt/CeO_2,[9] or in methanol synthesis over Cu/ZrO_2.[10] Therefore, the ability of the CeO_2-based supports to act as a hydrogen reservoir for chemical reactions adds interest to the investigation of the interaction of H_2 with these catalysts. In the case of ceria-containing systems, the ability to both spillover and store hydrogen strongly depends on the nature of the noble metal precursor, and also on the reduction/evacuation conditions.[11] When the catalyst is activated by a high temperature reduction (typically ≥500 °C) the intensity of these hydrogen transfer phenomena decreases, which may be interpreted as due to the inherent support dehydroxylation. It may also indicate the occurrence of some kind of strong metal−support interaction effect.[12] Recently, we have shown that H_2 chemisorption combined with HRTEM can successfully be applied to the characterization of a Rh/$Ce_{0.68}Zr_{0.32}O_2$ catalyst.[13] By using appropriate experimental conditions, the contribution of both the spillover species and the hydrogen species chemisorbed on the metal could be discriminated, and therefore, a rather simple technique could be fruitfully used for determining true rhodium dispersion values in these challenging catalytic systems.

In this work, the effect of different reduction treatments both on the metal nanostructure and particle size distribution and on the chemical behavior of Pt- and Pd-loaded $Ce_{0.68}Zr_{0.32}O_2$ catalysts are investigated by HRTEM and hydrogen chemisorption techniques. The comparison of the results presented here with those recently reported for a rhodium catalyst supported on the same ceria−zirconia mixed oxide sample[13] allows us to conclude that, as observed by some of our earlier studies,[7,14] the chemical deactivation caused by the increasing reduction temperatures are noble metal-sensitive, being stronger on Pt and Pd than on the corresponding Rh catalyst.

2. Experimental Section

NM/$Ce_{0.68}Zr_{0.32}O_2$ (NM: Rh, Pt, and Pd) catalysts were obtained from Rhodia. The Noble Metals were impregnated onto the support using $Rh(NO_3)_3$, $Pt[(NH_3)_4](NO_3)_2$, and $Pd[(NH_3)_4](NO_3)_2$ as precursors. The $Ce_{0.68}Zr_{0.32}O_2$ solid solution was from a previous study.[15] The impregnated precursors were dried at 110 °C and then calcined for 5 h in a flow of dry air at 450 °C.

* Corresponding author. Fax: +39-040-676-3903. E-mail: kaspar@univ.trieste.it.
† University of Trieste.
‡ University of Cádiz.
§ Current address: Department of Chemistry, University of Dundee, Dundee DD1 4HN, U.K.

10.1021/jp003632g CCC: $20.00
Published on Web 01/18/2001

Hereinafter these samples will be denoted Rh/CZ, Pt/CZ, and Pd/CZ. NM loading was 0.78 wt %, 0.55 wt %, and 0.53 wt % for Rh/CZ, Pt/CZ, and Pd/CZ, respectively. Characterization of the Rh/CZ catalyst was recently reported.[13] Before the experiments, an in situ cleaning procedure[16] was routinely applied in which the samples were heated in a flow of O_2(5%)/Ar (60 mL min^{-1}) at 550 °C for 1 h (initial heating rate 10 °C min^{-1}) then cooled to room temperature (rt), also under the oxidizing mixture.

The temperature-programmed reduction experiments (TPR-MS) were carried out on a conventional TPR system. A VG Sensorlab 200 quadrupole mass spectrometer equipped with Quasar Software 6.2 and PostSoft analysis software was used as the detector. The reduction profile was monitored by heating the sample (0.2 g, heating rate 10 °C min^{-1}) under a flow of H_2(5%)/Ar (25 mL min^{-1}) from room temperature to 1000 °C.

H_2 chemisorption and BET surface area measurements were conducted on a Micromeritics ASAP 2000 analyzer. A pressure change of less than 0.01% for 11 consecutive readings during a fixed equilibration time interval was chosen as a criterion for establishing the apparent equilibrium conditions. H_2 adsorption isotherms were measured at 25 °C and −80 °C in the H_2 pressure interval of 1−100 Torr. Adsorbed volumes were determined by extrapolation to zero pressure of the linear part of the adsorption isotherm. A chemisorption stoichiometry of H:NM = 1:1 was assumed.

The H_2 chemisorption studies were performed on the same sample, increasing progressively the reduction temperature (T_{red}). After the cleaning procedure, the samples (0.5 g) were reduced in a flow of H_2(5%)/Ar (60 mL min^{-1}) for 1 h at the selected reduction temperature and then evacuated for 4 h at 400 °C. To fully re-oxidize the ceria−zirconia support, a mild oxidation (MO) treatment was applied to the catalyst before each reduction step. This treatment consisted of heating the sample in a flow of O_2(5%)/Ar (60 mL min^{-1}) from −80 to 427 °C, followed by an immediate fast cooling to room temperature always in a flow of the oxidizing mixture. By following this procedure the support can be fully re-oxidized without appreciably modifying the metal dispersion.[14] In situ BET surface area measurements were carried out using the same equipment.

The transmission electron microscope used was a JEOL 2000 EX instrument equipped with a top-entry sample holder and an ion pump. This microscope, which operates at 200 kV, has a structural resolution of 0.21 nm. HRTEM micrographs of initial magnification up to ×600K were obtained using a film camera attached to the instrument. The resulting negatives were developed chemically and selected areas of the negatives were then digitized using a video camera interfaced to a computer running the SEMPER 6+ suite of image analysis software. Digital diffractogram patterns (DDPs) were obtained from these digitized images using the same software package.

Five 0.25−0.35 g samples each of the Pd/CZ and Pt/CZ catalysts were reduced by heating them at a rate of 10 °C min^{-1} to a reduction temperature of 150, 350, 500, 700, or 900 °C, and maintaining this temperature for a period of 1 h. After this reduction step, the samples were purged in pure He for 1 h at 500 °C or at the reduction temperature, if this was above 500 °C. The samples were then passivated by cooling the reactor tube in an acetone ice bath before switching the gas to O_2/He and allowing the sample to warm slowly to room temperature.[13,17] For study in the microscope, the samples were deposited from a hexane suspension prepared in an ultrasound bath onto Cu grids of holey carbon film by passing the grids repeatedly through the suspension using tweezers.

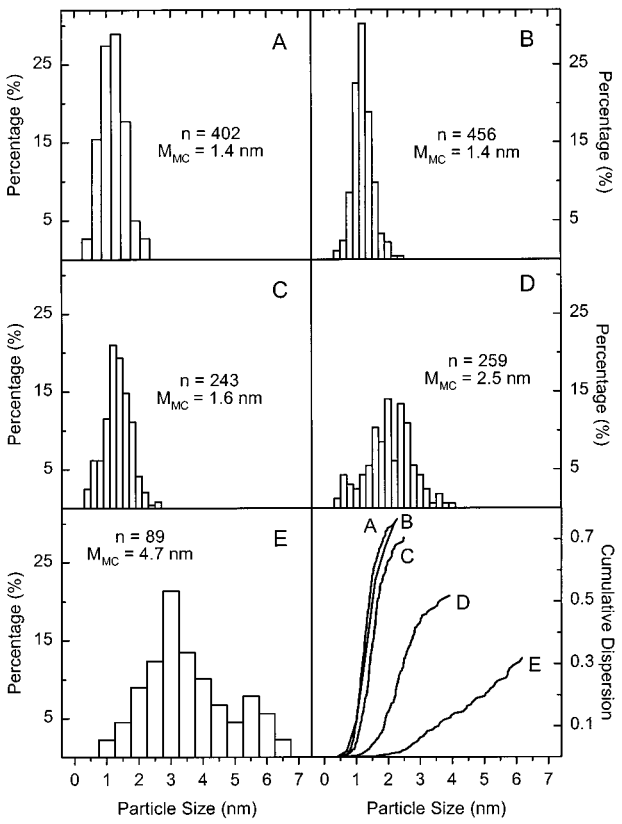

Figure 1. Pt particle size distribution histograms for $Pt/Ce_{0.68}Zr_{0.32}O_2$ samples reduced at 150 °C (A), 350 °C (B), 500 °C (C), 700 °C (D), and 900 °C (E). After reduction, samples were cooled and passivated as described in the text. Number of particles measured (*n*), mass-corrected mean particle size (M_{MC}), and cumulative dispersion plots are also included.

By measuring the size (defined as the longest visible width) of a large number of the metal particles from the HRTEM images in both planar and projection views,[14] particle size distributions and mean particle size data were obtained. Thus the effects of increasing reduction temperature on these factors could be studied. Further, this particle size data was used to estimate values for the dispersion of the metal phase. Dispersion is defined as the ratio of the number of metal atoms exposed at a particle surface (NM_S) to the total number of metal atoms present (NM_T), where NM is Pd, Pt, or Rh in this work. Cumulative dispersion curves were plotted using the particle size data by assuming a certain metal particle geometry (truncated cubooctahedron) and a certain orientation with respect to the oxide support (with {111}-type planes in contact at the interface, assuming fcc crystal structure for both the oxide and the metal[18]). The curves accumulate the contribution of metal particles to the dispersion with increasing particle size and so show the relative importance to the dispersion of different size ranges. The final value, therefore, gives the accumulated dispersion of all the particles measured, which is the estimated value of the overall dispersion for a particular sample.

3. Results and Discussion

3.1. HRTEM Microscopy Study. *3.1.1. Metal Particle Size and Dispersion.* Metal particle size distributions and cumulative metal dispersion curves obtained as explained above for the Pt/CZ and Pd/CZ samples after reduction at all five reduction temperatures are shown in Figures 1 and 2. The number of particles measured, *n*, and the mass-corrected mean particle size

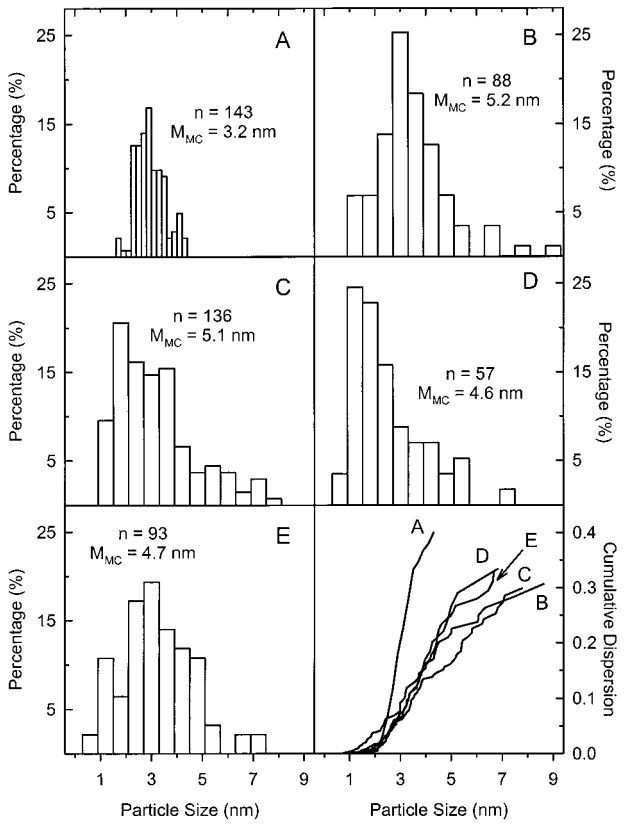

Figure 2. Pd particle size distribution histograms for $Pd/Ce_{0.68}Zr_{0.32}O_2$ samples reduced at 150 °C (A), 350 °C (B), 500 °C (C), 700 °C (D), and 900 °C (E). After reduction, samples were cooled and passivated as described in the text. Number of particles measured (*n*), mass-corrected mean particle size (M_{MC}), and cumulative dispersion plots are also included.

TABLE 1: Dispersion of the Noble Metal in NM/$Ce_{0.68}Zr_{0.32}O_2$ (NM = Pt, Rh, and Pd) Samples as Determined by HRTEM Microscopy[a]

	NM_S/NM_T		
reduction temp. (°C)	Pt/CZ	Rh/CZ	Pd/CZ
150	0.75	0.52	0.40
350	0.76	0.53	0.31
500	0.70	0.49	0.30
700	0.52	0.44	0.33
900	0.32	0.34	0.33

[a] Data for $Rh/Ce_{0.68}Zr_{0.32}O_2$ are from ref 13.

(based on the mass-fraction of each size range), M_{MC}, are also reported in these figures.

The Pt particles in these samples are plentiful, so large numbers of particles could be examined and a good statistical distribution obtained. It can be seen from Figure 1 that the particles are very small and that no significant changes were observed between T_{red} = 150 and T_{red} = 350 °C. However, as the temperature of reduction increased above 350 °C, particle size increased and the particle size distribution broadened, very slightly to T_{red} = 500 °C and then more significantly to T_{red} = 700 °C and T_{red} = 900 °C. This evolution with T_{red} is reflected in the cumulative dispersion curves in Figure 1. The Pt metal dispersion fell from the high values of 75−76% (for T_{red} = 150−350 °C) to 32% for T_{red} = 900 °C. The dispersion data are summarized in Table 1. Clearly, as in the case of the Rh/CZ samples,[13] the Pt/CZ samples appear to undergo a classic evolution with increasing reduction temperature resulting from the progressive sintering of the Pt particles. Indeed, probably due to the higher initial dispersion of Pt/CZ compared to Rh/CZ (0.75 vs 0.52, respectively), this evolution is more marked for the Pt samples than for the analogous Rh samples. Over the same reduction temperature range (150−900 °C) Rh dispersion falls from 52% to 34%.

The particle size distribution data reported in Figure 2 show that the Pd particles were much larger than those of Pt or of Rh. Also, Pd particles appeared to be very scarce on the oxide surface. Therefore, only relatively few could be measured. It should be noted here that because of the large difference in the bulk metal densities between Pt and Pd, the metal loadings used here for Pt (0.55 wt %) and Pd (0.53 wt %) should in fact result in the total volume of Pd present on the Pd/CZ catalyst being approximately twice that of Pt on Pt/CZ. In fact, it appears to be very much smaller.

In contrast to the results obtained for the Pt catalysts, the Pd particle size distributions and Pd dispersion data determined by HRTEM do not change significantly over the range from T_{red} = 350 °C to T_{red} = 900 °C. The slight deviation from this behavior noted in the case of the catalyst reduced at 700 °C may be due to the small statistical sample size, *n*, of particles measured in this case. The fact remains that significant metal particle sintering would normally be expected at $T_{red} \geq 500$ °C.

To account for the paucity of Pd particles detected by HRTEM, an attempt to obtain quantitative data on the distribution of the Pd metal over the oxide was made using a scanning electron microscope equipped with a EDS microprobe analysis system. This allowed EDS spectra of relatively small areas (about 1 μm square) of the powder sample to be obtained. In most spectra no Pd peaks were seen, only those of the $Ce_{0.68}Zr_{0.32}O_2$ mixed oxide. This is to be expected since the EDS method is not sensitive enough to detect elements present in amounts much lower than about 5 wt % and these catalysts contain a Pd loading of about 0.5 wt %. However, in a very few regions, strong Pd peaks were obtained, indicating local Pd concentrations of greater than 5 wt %. This suggested that the metal was very heterogeneously distributed with high concentrations in certain points but very low levels generally. The HRTEM results might therefore be explained as being characteristic of the majority of the surface area of the sample where very low concentrations of Pd particles were found, while a large amount of the total mass of the Pd metal was concentrated in a few small regions, perhaps in the form of relatively very large particles. Since the particle size distributions and HRTEM dispersion values relate solely to the Pd-poor regions of the sample, the independence of these data of T_{red} may be explained by the large distances between particles in these regions, the particles being effectively isolated from each other and unable to coalesce during the 1 h reduction treatments. We favor this explanation of this unusual apparent lack of sintering upon increasing the reduction temperature, even though other explanations cannot be excluded.

3.1.2. Metal Particle Morphology. HRTEM images of metal particles in the above samples were examined, and representative images are presented in Figures 3 and 4. Metallic Rh, Pt, and Pd have the fcc structure with unit cell lengths of 0.380, 0.392, and 0.389 nm, respectively. For metallic Pd and Pt, this gives rise to interplanar spacings, **d**, for the planes of type {200} and {111} of approximately 0.195 and 0.225 nm for Pd; and 0.190 and 0.220 for Pt, respectively. Under normal working conditions, the {111} spacing is the only one that can be routinely detected by the microscope used, although detection of the {200} spacing is also possible under favorable operating and experimental conditions. Previous work[19] has shown that the $Ce_{0.68}Zr_{0.32}O_2$

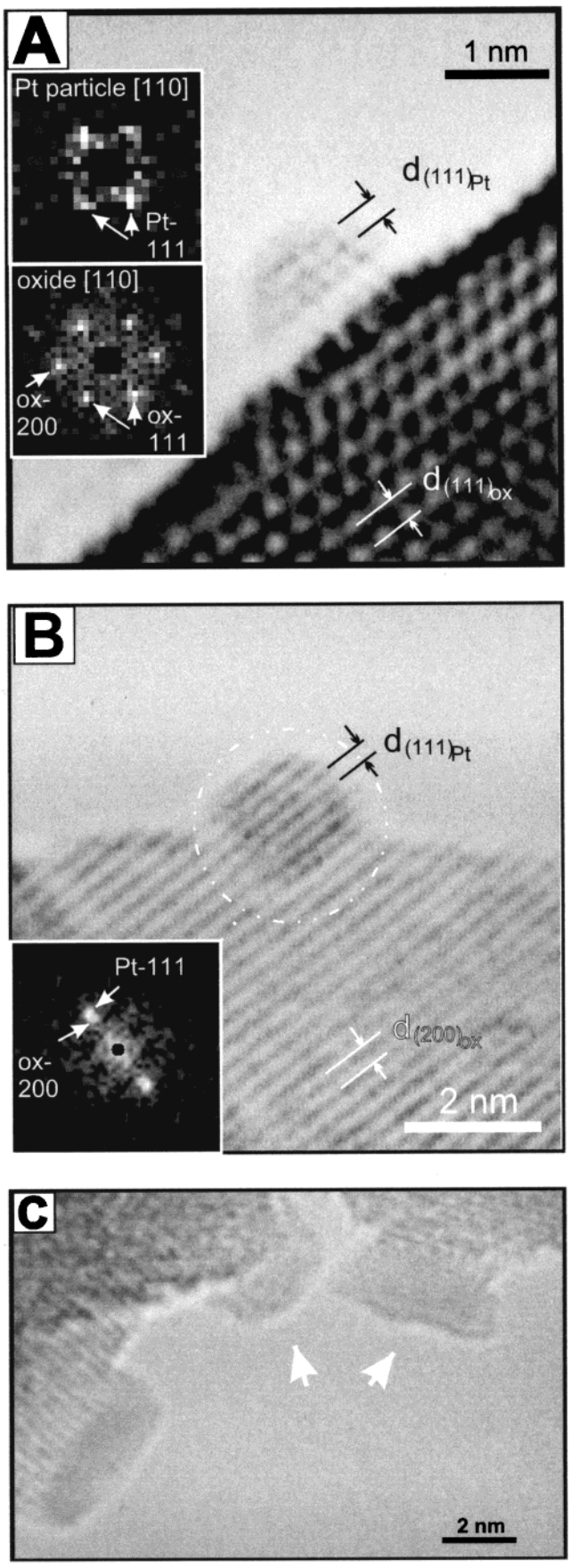

Figure 3. Typical HRTEM images and Digital diffractograms (DDPs) recorded for the $Pt/Ce_{0.68}Zr_{0.32}O_2$ sample reduced at 500 °C (A), 700 °C (B), and 900 °C (C).

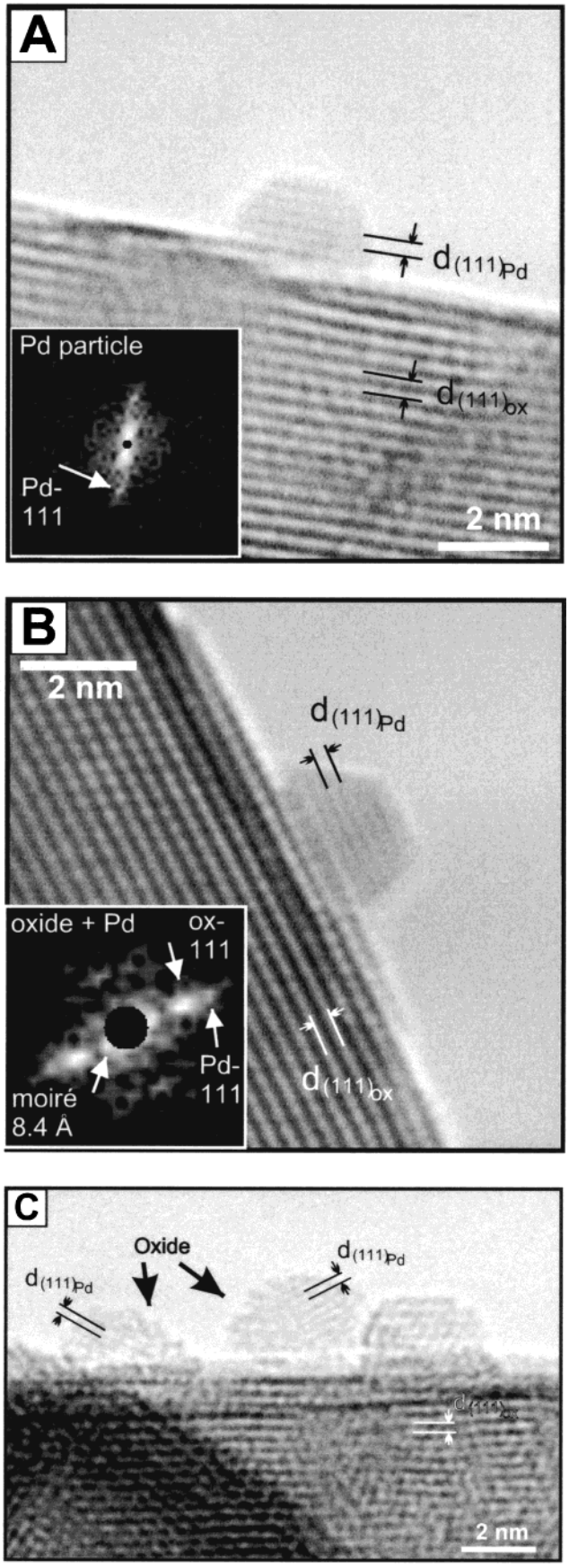

Figure 4. Typical HRTEM images and digital diffractograms (DDPs) recorded for the $Pd/Ce_{0.68}Zr_{0.32}O_2$ sample reduced at 350 °C (A), 500 °C (B), and 900 °C (C).

bare oxide support contains a significant amount of tetragonal phase. However, to allow simple comparisons between the fcc

metal structure and that of the oxide the oxide crystallography is also expressed here in terms of fcc symmetry.

As shown in Figure 3A for a sample reduced at 500 °C, the Pt particles in the Pt/CZ samples generally exhibit the regular truncated cubooctahedron shape which has been found to be typical for Rh/CeO_2 catalysts.[17] Although the small size of the particles tends to limit the amount of information available, it was still possible to generate meaningful digital diffractogram patterns (DDPs) of the Pt particle (top) and the $Ce_{0.68}Zr_{0.32}O_2$ support (bottom) from this image. The Pt and the oxide are viewed along their respective [110] zone axes. Spots in the DDPs can be assigned to {111}- and {200}-type planes in the oxide support and {111}-type in the Pt particle. Both visible (111) planes in the oxide and in the metal particle are aligned since the corresponding spots in the DDPs are at the same angles. Further, the metal particle is seen to be in contact with the underlying oxide at a shared (111) plane. This validates the assumptions made in estimating metal dispersion values from particle size data described above. In the same material reduced at $T_{red} = 700$ °C, the metal particles maintain their regular shape and there is still no evidence of decoration of the metal particle by the oxide. Such a particle is shown in Figure 3B. In this case, as was found in a minority of cases, the visible (111) planes of the Pt metal are aligned, not with (111) planes, but with (200) planes of the $Ce_{0.68}Zr_{0.32}O_2$ support since the corresponding spots in the DDP are collinear. After reduction at $T_{red} = 900$ °C, apparently regular particles continue to be observed with Pt-(111) planes aligned with either the (111) or (200) planes of the oxide. However, in a minority of particles there is evidence of movement of material from the support oxide onto the Pt particles (decoration). An example is given in Figure 3C where two particles (arrowed) with irregular shapes are seen. These irregularities are likely to be caused by the decoration of the metal particles by the reduced support.

The Pd crystals in Pd/CZ are larger, and therefore, less difficult to image in HRTEM. Figure 4 presents images of Pd particles typical of those observed in the samples reduced at $T_{red} = 150-900$ °C. Figure 4A contains an image obtained for the sample reduced at 350 °C. The main contrast lines in the oxide and in the metal are clearly aligned in the HRTEM image. In the DDP of the metal particle (inset) these contrasts give rise to a spot which can be assigned to {111}-type planes of the Pd metal. These planes are aligned with the visible planes of the oxide support, which are also {111}-type. The same orientation between the Pd particle and the oxide support is also observed in the sample reduced at $T_{red} = 500$ °C (Figure 4B). Generally, this was found to be the case for the range of reduction temperature up to 700 °C as was the regular truncated cubooctahedral morphology of the particles and the absence of evidence of decoration of the Pd by the support oxide. However, turning to the Pd/CZ sample reduced at $T_{red} = 900$ °C, we find Pd particles which are often of irregular shape with disordered distributions of atoms on some of their exposed surfaces, although regular particles are also still observed. Decoration effects are evident in Figure 4C. Two of the particles consist of a region of small inter-planar spacing, which can be assigned as {111}-type Pd planes, as well as a somewhat disordered region of rounded profile with larger interplanar spacings. This appears to be composed of oxide material transported from the $Ce_{0.68}Zr_{0.32}O_2$ support to form a decorating layer over part of the Pd particle.

The proportion of decorated particles in the Pt/CZ and Pd/CZ samples reduced at $T_{red} = 900$ °C were estimated to be less than 5% in both cases.

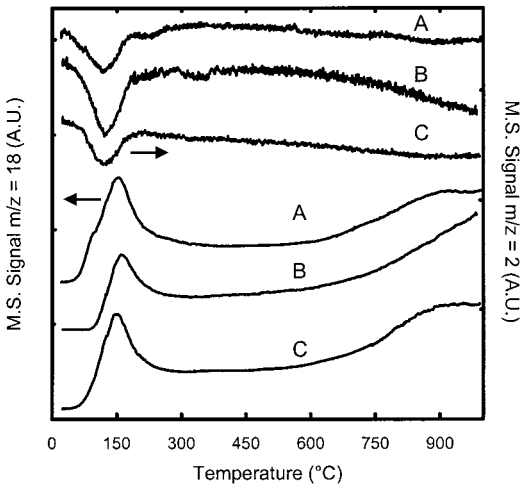

Figure 5. TPR-MS profiles for fresh $Rh/Ce_{0.68}Zr_{0.32}O_2$ (A), $Pt/Ce_{0.68}Zr_{0.32}O_2$ (B), and $Pd/Ce_{0.68}Zr_{0.32}O_2$ (C): H_2 uptake (upper traces) and H_2O evolution (lower traces).

3.2. TPR-MS Study. The TPR-MS profiles for H_2 uptake and H_2O evolution of Pt/CZ and Pd/CZ samples after the cleaning procedure are reported in Figure 5. For the sake of comparison the profile obtained for Rh/CZ is included. Irrespective of the nature of the NM, the H_2 uptake is characterized by an intense and broad peak with maximum around 125 °C and a shoulder at a higher temperature is found in Rh/CZ and Pt/CZ. In addition, a very broad and poorly resolved H_2 uptake may be noted at the highest temperature region. This latter effect is more intense in the Pt/CZ catalyst. The overall appearance of the profiles is similar to those previously reported for some other ceria−zirconia supported noble metal catalysts.[7] Accordingly, we attribute these features to processes involving the reduction of the noble metal oxide and the support.[20] The low-temperature peaks can be attributed to the reduction of the dispersed metal phase and a partial reduction of the support. The high-temperature features can be associated to the processes of deep reduction in the bulk of the ceria−zirconia solid solution. Of note is the delay in H_2O production with respect to the H_2 uptake, which occurred for all the catalysts, and was particularly large for the Pt/CZ sample. Even though some delay in water production is observed in our system due to retention of H_2O in the heated transfer line, the observed features are consistent with a reduction process of the support, which occurs via an initial H_2 adsorption, which then leads to creation of oxygen vacancies.[8,21,22] The observation of two main reduction process at about 150 °C and above 650 °C, with a maximum at/above 900 °C is particularly relevant to this study. Notice that NM decoration by the support was observed by HRTEM only at the highest reduction temperature investigated, i.e., 900 °C, which could suggest some correlation between the two phenomena.

3.3. H_2 Chemisorption. As shown for Rh/CZ in the previous paper,[13] the low-temperature H_2 chemisorption, which was proposed for estimation of NM (NM = Rh, Pt) dispersion in CeO_2 systems,[14] can be successfully extended to Rh/CeO_2-ZrO_2 mixed oxides, its extension to Pt being the subject of this study. As far as the Pd/CeO_2 systems are concerned, the situation is less clear. This is due to the fact that this noble metal easily forms bulk hydrides under the chemisorption conditions usually employed for characterizing Pt and Rh catalysts.[23] Accordingly, a number of alternative chemisorption routines have been developed, the major aim of which was to minimize hydride formation (see for example refs 24−26).

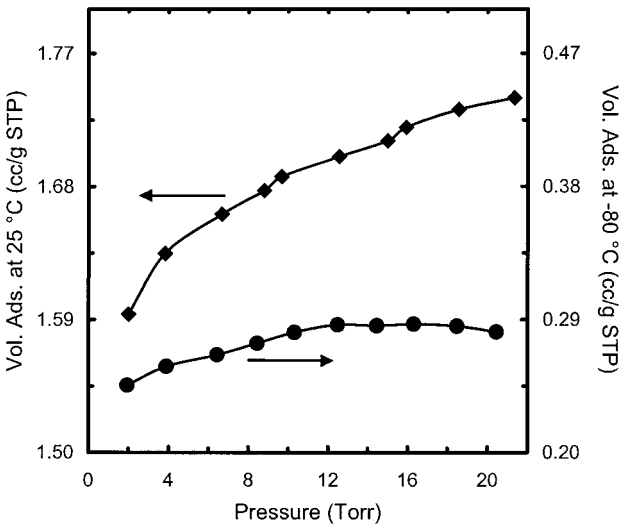

Figure 6. Typical H_2 adsorption isotherm measured at −80 and 25 °C on $Pt/Ce_{0.68}Zr_{0.32}O_2$ reduced at 150 °C.

TABLE 2: Volumetric Study of Hydrogen Chemisorption on $Pt/Ce_{0.68}Zr_{0.32}O_2$

run[a]	reduction temp. (°C)	H/Pt_T 25 °C	H/Pt_T −80 °C
1	150	5.20	0.85
2	350	1.11	0.62
3	150[b]		0.83
4	500	0.42	0.42
5	150[b]		0.75
6	700	0.23	0.26
7	150[b]		0.40
8	900		0.10
9	150[b]		0.19
10	150[c]		0.47

[a] Catalyst evacuated at 400 °C for 4 h before chemisorption measurement. [b] Catalyst from previous experiment, re-oxidized in flow of O_2 (5%)/Ar from −80 to 427 °C, heating rate 10 °C min^{-1}. [c] Catalyst from previous experiment, re-oxidized in flow of O_2 (5%)/Ar from −80 to 700 °C, heating rate 10 °C min^{-1}. $Pt_s/Pt_t = 0.72$ was detected by HRTEM.

3.3.1. $Pt/Ce_{0.68}Zr_{0.32}O_2$ Catalyst. Adsorption isotherms obtained at −80 and 25 °C on Pt/CZ reduced at 150 °C are reported in Figure 6. The approximately 5-fold increase in the amount of hydrogen adsorbed at 25 °C compared to that determined at −80 °C indicates that spillover of H-species onto the support represents a very significant contribution at room temperature. As pointed out in the previous study on Rh/CZ,[13] under our experimental conditions the occurrence of spillover phenomena leads to long equilibration times, particularly at low H_2 pressures. This is due both to the use of a restrictive equilibrium criterion, as described in the Experimental Section, and to the fact that at room temperature. spillover of H-species is a slow process, because of its activated nature.[21,27] Table 2 summarizes the quantitative results of the study of H_2 adsorption on Pt/CZ.

A perusal of data reported in Table 2 reveals a number of interesting features: (i) The H/Pt ratio measured at −80 °C steeply decreases with the reduction temperature; (ii) for reduction temperatures ≥500 °C very similar H/Pt ratios are measured at −80 and 25 °C. Also, comparable equilibration times are observed in the two measurements; (iii) reoxidation at 427 °C and subsequent reduction at 150 °C leads to a significant increase of H/Pt measured at −80 °C.

No appreciable decrease of BET surface areas has been induced by the treatments reported in Table 2, as confirmed by in situ surface area measurements after the cleaning treatment (21.2 $m^2\ g^{-1}$) and run nine, as reported in Table 2 (20.9 $m^2\ g^{-1}$).

Generally speaking, the data obtained on the Pt/CZ broadly follow those observed on the Rh/CZ in that an increase of the reduction temperature leads to a decrease of the extent of hydrogen spillover. This is clearly demonstrated both by the consistency of the H/Pt values measured at 25 and at −80 °C and by the fact that comparable equilibration times are obtained at the two adsorption temperatures, in the absence of spillover phenomena. The latter is a remarkable observation which represents an independent criterion for detecting the occurrence of spillover under our experimental conditions. By applying the criterion described in the Experimental Section, the measurements performed at −80 °C allowed us to estimate an average time for reaching the apparent equilibrium at 2 Torr of H_2 of 17.9 ± 3.9 min for Rh/CZ, and 16.2 ± 3.9 min for Pt/CZ. This means that, under our experimental conditions, the average equilibrium time is approximately the same, 17 min, for the two noble metals. Equilibration times significantly longer than 17 min would therefore indicate the occurrence of hydrogen spillover. Such is the case for the time determined, at 25 °C, for the chemisorption of hydrogen on the Pt/CZ catalyst reduced at 150 °C for which a value of 700 min was measured.

In Figure 7 we plot the ratio between the metal dispersion data as determined by hydrogen chemisorption at −80 °C (H/NM_t) and by HRTEM (NM_s/NM_t), i.e.: $[(H/NM_t)/(NM_s/NM_t)] = (H/NM_s)$, versus the reduction temperature, for the Pt/CZ and Rh/CZ catalysts. This plot allows us to detect rather easily any loss of the metal chemisorption capability due to phenomena other than metal sintering. In effect, if metal deactivation occurs, the values for metal dispersion determined from volumetric adsorption would become smaller than those estimated by HRTEM, and therefore H/NM_s values <1 would be obtained.

There are a number of aspects worth outlining from the analysis of Figure 7. First, upon increasing the reduction temperature, the H/NM_s ratio progressively decreases, thus indicating the occurrence of some deactivation of both Rh and Pt. As already noted in ref 13 for Rh/CZ, the high textural stability of these catalysts, the surface area of which remain practically constant over the whole range of reduction temperatures, allows us to reasonably exclude the metal encapsulation associated with the sintering of the support as the likely origin of the observed effect. Accordingly, it should be interpreted as due to the onset of a strong metal/support interaction phenomenon similar to that described in ref 14 for Pt/CeO_2 catalysts.

The comparison of the evolution with T_{red} of the H/NM_s ratios for Rh/CZ (Figure 7A) and Pt/CZ (Figure 7B) leads to an additional remarkable observation: the sensitivity of Rh and Pt to the chemical deactivation induced by the increase of T_{red} is significantly different, being much larger in the case of the latter. Differences may be noticed in terms of the variation of H/NM_s with T_{red}, i.e., in the intensity of the deactivation phenomena, but also in the reduction temperature at which the loss of chemisorptive capability starts to be observed, 350 °C in the case of Pt, and much higher, 700 °C, on Rh/CZ. In this latter respect, it is worth recalling that temperatures around 350 °C are routinely employed to reduce the platinum catalysts before chemisorption measurements. Our results show that, in the case of the Pt/CZ catalysts, this temperature is too high to ensure a meaningful determination of the metal dispersion by using hydrogen chemisorption techniques. However, the results reported in Figure 7 show that H_2 chemisorption at −80 °C may be fruitfully used to estimate the metal dispersion in Pt/

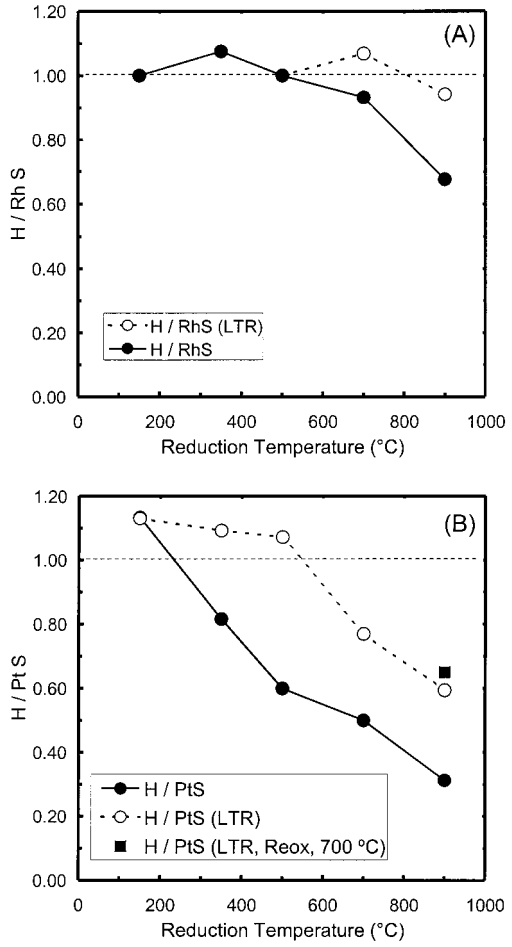

Figure 7. Ratio between metal dispersion data as determined from H_2 chemisorption (H/NM_t) and as determined by HRTEM (NM_s/NM_t): $(H/NM_t)/(NM_s/NM_t) = H/NM_s$, for Rh/$Ce_{0.68}Zr_{0.32}O_2$ (data from ref 13) (A) and Pt/$Ce_{0.68}Zr_{0.32}O_2$ (B). (●) Samples reduced at the indicated temperatures, (○) samples reduced at the indicated temperatures, then re-oxidized at 427 °C and further rereduced at 150 °C (LTR), (■) Sample reduced at 900 °C, then re-oxidized at 700 °C and further rereduced at 150 °C (LTR).

CZ catalysts reduced at 150 °C, a procedure which might be proposed as a convenient routine for this purpose.

Figure 7 also shows that the chemisorptive capability of the deactivated catalysts may be recovered by a relatively mild oxidation at 427 °C followed by rereduction at 150 °C. This regeneration effect is practically complete in the case of Rh/CZ, independent of T_{red}. By contrast, for Pt/CZ catalysts reduced at 700 °C or 900 °C, the recovery is only partial. Moreover, in the case of Pt/CZ samples reduced at 900 °C, its complete regeneration could not be achieved even by applying a much harder reoxidation treatment, at 700 °C. These observations also support the existence of differences in the nature of the interactions occurring between the ceria−zirconia mixed oxide and the two metals considered here, Pt and Rh. These findings appear to be consistent with some previous observations on Pt/CeO_2[14] and Rh/CeO_2[11] systems, in which the sensitivity of these two metals to the chemical deactivation effects induced by increasing reduction temperatures are somewhat different, being higher in the case of Pt. Also in agreement with the results reported here for Pt/CZ, reoxidation of a deactivated Pt/CeO_2 followed by a low temperature reduction treatment does not allow the catalyst to fully recover its chemisorptive capability.[14] Accordingly, in terms of the nature of the metal/support interaction effects, clear analogies seem to exist between NM/CeO_2 and NM/CZ catalysts.

TABLE 3: Volumetric Study of Hydrogen Chemisorption on Pd/$Ce_{0.68}Zr_{0.32}O_2$

run[a]	reduction temp. (°C)	equilibrium time (min.)[b]	H/Pd_T[c]
1	150	1510	2.15
2	350	47	0.28
3	500	23	0.17
4	700	23	0.07
5	150[d]	1152	2.00
6	900	13	0.05
7	150[d]	54	0.10

[a] Catalyst evacuated at 400 °C for 4 h before chemisorption measurement. [b] Time to reach equilibrium at H_2 pressure of 2 Torr. [c] Values obtained by extrapolation to zero of the linear part of the isotherm in the range of pressure below 12 Torr. [d] Catalyst from previous experiment, re-oxidized in flow of O_2 (5%)/Ar from −80 to 427 °C, heating rate 10 °C min^{-1}.

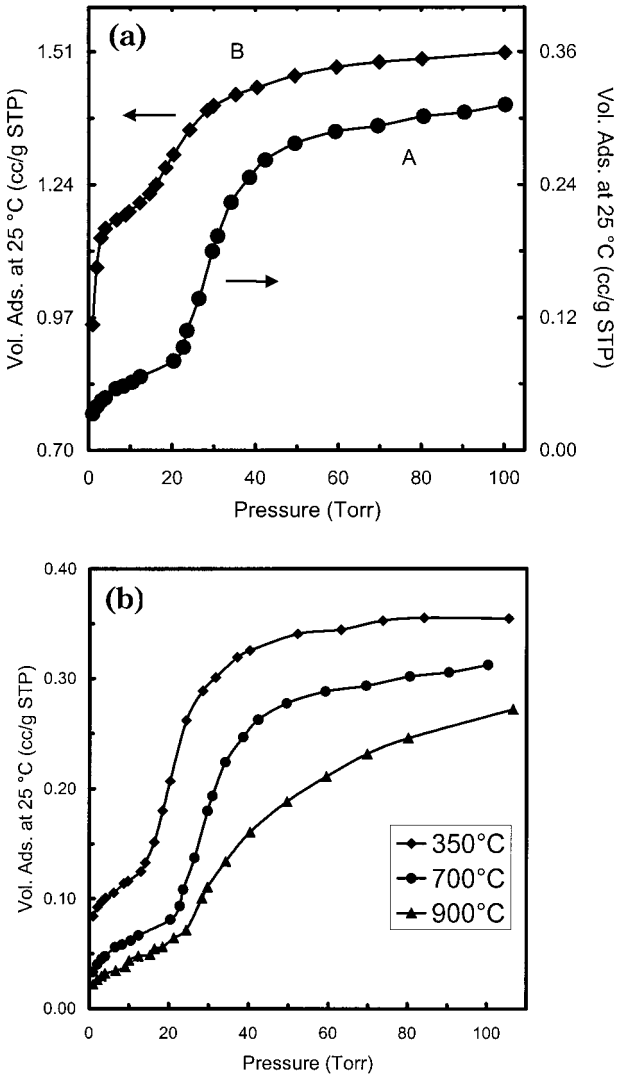

Figure 8. Typical H_2 adsorption isotherm obtained at 25 °C on (a) Pd/$Ce_{0.68}Zr_{0.32}O_2$ reduced at 700 °C (A) and the same sample oxidized at 427 °C and rereduced at 150 °C (B); (b) effect of the reduction temperature on the H_2 adsorption isotherms.

3.3.2. Pd/$Ce_{0.68}Zr_{0.32}O_2$ Catalyst. Typical H_2 adsorption isotherms obtained for Pd/CZ after reduction treatments as reported in Table 3, are presented in Figure 8. Two distinct regions are clearly discerned in the shape of the isotherms, thus indicating that an additional chemisorption process occurs at H_2 pressures higher than 12 Torr. This process, which is absent

in both Pt/CZ and Rh/CZ catalysts, is associated with the formation of a bulk palladium hydride.[23] As mentioned above, the choice of experimental conditions for investigating H_2 chemisorption on palladium catalysts is critically important in order to prevent hydride formation. H_2 pressures in the range 2−10 Torr are typically recommended as appropriate for measuring the Pd dispersion.[24,26] At higher H_2 pressures (100−400 Torr), the use of high temperatures (100 °C) is necessary to prevent hydride formation. Because of the very likely occurrence of hydrogen spillover, however, the latter experimental conditions cannot be applied to the characterization of Pd/CeO_2-ZrO_2 catalysts.[28] In accordance with some preliminary experiments carried out on a Pd/Al_2O_3 catalyst, chemisorption studies at −80 °C and at low P_{H_2} (<10 Torr), cannot be applied either because of hydride formation. The occurrence of this undesirable side process could be deduced from the comparison of H/Pd ratio (>1) determined under the conditions mentioned above, with the CO/Pd value (0.34) estimated from a conventional volumetric procedure.[25] Very recently, an experimental procedure has been developed which allows meaningful H/Pd values for a $Pd/Ce_{0.6}Zr_{0.4}O_2/Al_2O_3$ catalyst to be obtained.[25] This procedure consists of performing the isotherm at room temperature and low P_{H_2} (<10 Torr) on a catalyst sample which, after reduction, had been submitted to a prolonged evacuation treatment (up to 20 h) at 400 °C. In this way, as already reported for Rh/CeO_2,[11] the spillover process could be blocked, thus making its contribution to the total amount of chemisorbed hydrogen negligible. It should be noted, however, that prolonged evacuation times at 400 °C may induce some metal sintering. Likewise, some unpublished data from our laboratory for a $Pt/Ce_{0.6}Zr_{0.4}O_2/Al_2O_3$ catalyst suggest that spillover of hydrogen may be less effective in the alumina-supported system than in NM/CZ catalysts. Finally, attempts to apply pulse chemisorption techniques to the determination of the NM dispersion in NM/CZ catalysts were also fruitless.[13] To summarize, the development of a procedure allowing the use of hydrogen as a probe molecule for determining Pd dispersion in Pd/CZ systems represents a challenging and, as yet unresolved, problem.

As can be seen in Figure 8a, below 12 Torr, the adsorption isotherms show a plateau. This plateau is observed on the isotherms recorded for all the Pd samples. It is worth noting, however, that the inflection point which delimits the second part of the isotherms, the one associated with hydride formation, shifts toward higher P_{H_2} values on increasing the reduction temperature. Accordingly, the H/Pd_T values were obtained by extrapolation to zero pressure of the linear part of the isotherms in the range of 2−12 Torr. Table 3 summarizes the results obtained for all the Pd/CZ samples.

As already noted for Pt/CZ (Table 2) the H/Pd data in Table 3 are also strongly affected by the reduction temperature. For the catalysts reduced at 150 °C, H/Pd exceeds unity, thus indicating the occurrence of significant H-spillover. This is unequivocally confirmed by the very long equilibration time (1510 min) determined for this sample. A reduction temperature as low as 350 °C is able to dramatically decrease both the H/Pd ratio and the equilibration time. However, the latter value is still significantly larger (47 min) than that reported above (17 min) for a chemisorption process occurring only on the noble metal. It could be argued that different NM and experimental conditions are employed for the Pd/CZ compared to Rh/CZ and Pt/CZ. However, the equilibration times determined on the Pd/CZ catalysts reduced at 500−900 °C (Table 3, runs 3, 4, and 6), for which the spillover phenomena are likely to be suppressed, are very close to the value (17 min) reported above for Rh and Pt. We may conclude, accordingly, that the criterion for detecting the existence of spillover applied to Rh/CZ and Pt/CZ catalysts can be extended to the Pd-containing system. This is a remarkable observation since, to our knowledge, for the first time, an independent criterion for detecting hydrogen spillover in Pd/CeO_2-containing catalyst is reported. There is strong interest in the use of Pd-based technology in automotive pollution control due to the ability of Pd catalysts to promote CO and hydrocarbon oxidation at low temperatures.[29]

The isotherm obtained for the sample reduced at 700 °C, oxidized at 427 °C, and further reduced at 150 °C (Figure 8, trace B) deserves some further comment. In fact, in this case also, a plateau corresponding to hydride formation is observed at 10−20 Torr of H_2. However, the extrapolation of the linear part of the isotherm (10−20 Torr) to zero pressure leads to a value of H/Pd = 2.0. This indicates that, under our experimental conditions, hydrogen spillover onto the support takes place before the metal becomes saturated. Under these circumstances no true H/Pd ratios may be determined.

The apparent exposed metal surface area continuously drops as the reduction temperature is increased. After reduction at 900 °C, a H/Pd_T ratio as low as 0.05 is observed. It is known that Pd may be irreversibly encapsulated into a CeO_2 support.[29] As expected, the effect is particularly strong in the case of high-surface-area ceria samples.[30] In our case, however, as deduced from the in situ surface area measurements carried out on the fresh Pd/CZ catalyst (20.4 $m^2\ g^{-1}$), and after reduction at 900 °C (20.3 $m^2\ g^{-1}$), the textural changes are negligible. Therefore, metal encapsulation due to the collapse of the surface area should not be a relevant factor in explaining the observed loss of chemisorption capability. Likewise, the HRTEM studies have provided experimental evidence of metal decoration effects. This phenomenon, which affects a relatively small fraction of the total number of metal particles (<5%), was only observed at the highest reduction temperature, 900 °C. Deactivation effects, however, are noticeable on the sample reduced at 700 °C, thus suggesting that factors other than decoration are relevant.

Due to the difficulties discussed above in obtaining reliable Pd dispersion data from the HRTEM study, the relationship existing between the decrease of the H/Pd ratio and the sintering of the metal remains uncertain. It should be noted, however, that the shift toward higher P_{H_2} pressures occurred in the inflection point of the isotherms reported in Figure 8b. This shift, which indicates a progressive decrease in the stability of the palladium hydride as the reduction temperature is increased, might well be interpreted as due to some Pd sintering.[31] However, the occurrence of some perturbations in the electronic properties of the metal particles cannot be discounted. In this respect, it is worth recalling that, as shown in Table 3, a mild reoxidation at 427 °C, and subsequent reduction at 150 °C, leads to an appreciable increase of both H/Pd_T ratios and equilibration times. Since the reoxidation temperature applied here is moderate, it is unlikely that the reactivation of the Pd/CZ occurs entirely through re-dispersion of the Pd and/or destruction of decorating layers.[14] Therefore, this change in the chemisorptive behavior, which is associated with partial or complete recovery of both hydrogen adsorption on the metal and spillover onto the support, suggests that electronic metal−support interaction effects play a major role in determining the chemisorptive behavior of the Pd/CZ catalyst, even though some contribution due to metal sintering and subsequent re-dispersion cannot be disregarded.

4. Conclusions

The combination of HRTEM and hydrogen chemisorption techniques have been fruitfully applied to the characterization of NM/CZ catalysts. By using the metal dispersion data determined from HRTEM as a reference, we have developed a simple H_2 chemisorption protocol allowing reliable platinum dispersion data to be obtained. As revealed by the time required to reach an apparent chemisorption equilibrium, −80 °C is a temperature low enough as to avoid the spillover contribution to the total amount of adsorbed hydrogen. Under these conditions, a good agreement is found between the H/M_t values determined from the volumetric adsorption measurements, and the M_s/M_t data deduced from the analysis of the HRTEM micrographs. A good correlation between H/M_t and M_s/M_t ratios could only be observed on Pt/CZ catalysts reduced at $T_{red} <$ 350 °C. For $T_{red} \geq$ 350 °C, H/M_t was always smaller than the corresponding M_s/M_t value, the deviation progressively increasing with the reduction temperature. This effect is interpreted as being due to the onset of a significant metal/support interaction effect, as a result of which, a partial loss of the Pt chemisorption capability occurs. Depending on T_{red}, the deactivated catalyst may be fully or only partly regenerated by a relatively mild reoxidation treatment at 427 °C followed by reduction at 150 °C. This observation lends further support to the interpretation suggested above.

Both the reduction temperature at which the loss of chemisorption capability of the Pt/CZ sample starts to be observed, and the magnitude of the drop in the H/NM_t values contrast with those reported earlier for a Rh catalyst supported on the same ceria−zirconia mixed oxide sample, the deactivation effect being much stronger on the former. This suggests that the effect is sensitive to the noble metal used, and therefore, that the selection of the reduction conditions is a key experimental parameter for obtaining reliable metal dispersion data by means of the proposed chemisorption technique.

Regarding the Pd/CZ catalyst, the formation of a bulk hydride as well as the uneven distribution of the metal, with the resulting uncertainty in the particle size distributions determined by HRTEM, introduce some very severe additional difficulties in devising a protocol for obtaining meaningful metal dispersion data from H_2 volumetric measurements. Despite these drawbacks, some conclusions may be outlined from this study. First, the H/Pd_t values determined at 25 °C and $P_{H_2} <$ 10 Torr, as well as the long times required to reach an apparent equilibrium under the conditions described above, indicate that spillover also plays an important role in the chemistry of the H_2−(Pd/CZ) system. Likewise, the evolution of the H/Pd_t ratio with T_{red}, as well as the recovery of the chemisorption capability induced by the reoxidation (427 °C)/reduction (150 °C) treatment clearly indicates that metal/support interaction effects have a strong influence on the chemical behavior of the Pd/CZ catalyst. Though the T_{red} value at which deactivation starts to be noticeable could not be established precisely, the results reported here suggest that the behavior of Pd is close to that exhibited by platinum, and therefore, that rhodium is by far the least sensitive metal to the deactivation effects caused by the interaction of the NMs with the reduced ceria−zirconia mixed oxide support.

In addition to the metal particle size distribution data, HRTEM has provided valuable information about the nanostructural properties of the NM/CZ (NM: Pt, Pd) systems. In this respect, it was found that that both Pd and Pt particles grow on the CZ support in accordance with some well-defined structural relationships, the characteristics of which are established in the text. Likewise, we have been able to provide the very first direct evidence of metal decoration in ceria−zirconia mixed oxide-supported Pd and Pt catalysts. Decoration of the metal particles by the reduced support could only be observed at the highest reduction temperatures (900 °C). Even under these very severe conditions, a limited fraction of the imaged metal particles appear decorated, suggesting that geometric factors play a secondary role in determining the hydrogen chemisorptive properties of these catalysts.

Acknowledgment. The present paper has received financial support from the TMR Program of the European Commission (Contract FMRX-CT-96-0060). Financial support from University of Trieste, the Regione Friuli Venezia-Giulia, Fondo regionale per la ricerca L.R. 3/1998, Fondo Trieste 1999, the CICYT (Project No. MAT99-0570), and the Junta de Andalucía are also acknowledged. HRTEM images were recorded at the Electron Microscopy facilities of UCA.

References and Notes

(1) *Recent Progress in Catalysis by Ceria and Related Compounds*; Bernal, S., Kašpar, J., Trovarelli, A., Eds.; Elsevier Science: Amsterdam, 1999; *Catal. Today*, vol. 50, pp 173−443 and refs therein.
(2) Zamar, F.; Trovarelli, A.; de Leitenburg, C.; Dolcetti, G. *J. Chem. Soc. Chem. Commun.* **1995**, 965.
(3) Trovarelli, A. *Catal. Rev.—Sci. Eng.* **1996**, *38*, 439.
(4) Murota, T.; Hasegawa, T.; Aozasa, S.; Matsui, H.; Motoyama, M. *J. Alloys Compd.* **1993**, *193*, 298.
(5) Ozawa, M.; Kimura, M.; Isogai, A. *J. Alloys Compd.* **1993**, *193*, 73.
(6) Madier, Y.; Descorme, C.; LeGovic, A. M.; Duprez, D. *J. Phys. Chem. B* **1999**, *103*, 10999.
(7) Fornasiero, P.; Kašpar, J.; Sergo, V.; Graziani, M. *J. Catal.* **1999**, *182*, 56.
(8) Bernal, S.; Calvino, J. J.; Cifredo, G. A.; Rodriguez-Izquierdo, J. M.; Perrichon, V.; Laachir, A. *J. Chem. Soc., Chem. Commun.* **1992**, 460.
(9) Otsuka, K.; Wang, Y.; Sunada, E.; Yamanaka, I. *J. Catal.* **1998**, *175*, 152.
(10) Jung, K.-D.; Bell, A. T. *J. Catal.* **2000**, *193*, 207.
(11) Bernal, S.; Calvino, J. J.; Cifredo, G. A.; Laachir, A.; Perrichon, V.; Herrmann, J. M. *Langmuir* **1994**, *10*, 717.
(12) Cunningham, J.; O'Brien, S.; Sanz, J.; Rojo, J. M.; Soria, J.; Fierro, J. L. G. *J. Mol. Catal.* **1990**, *57*, 379.
(13) Gatica, J. M.; Baker, R. T.; Fornasiero, P.; Bernal, S.; Blanco, G.; Kašpar, J. *J. Phys. Chem. B* **2000**, *104*, 4667.
(14) Bernal, S.; Calvino, J. J.; Cauqui, M. A.; Gatica, J. M.; Larese, C.; Omil, J. A. P.; Pintado, J. M. *Catal. Today* **1999**, *50*, 175.
(15) Colon, G.; Pijolat, M.; Valdivieso, F.; Vidal, H.; Kašpar, J.; Finocchio, E.; Daturi, M.; Binet, C.; Lavalley, J. C.; Baker, R. T.; Bernal, S. *J. Chem. Soc., Faraday Trans.* **1998**, *94*, 3717.
(16) Daturi, M.; Binet, C.; Lavalley, J. C.; Vidal, H.; Kašpar, J.; Graziani, M.; Blanchard, G. *J. Chim. Phys.* **1998**, *95*, 2048.
(17) Bernal, S.; Botana, F. J.; Calvino, J. J.; Cifredo, G. A.; Perez-Omil, J. A. *Catal. Today* **1995**, *23*, 219.
(18) Bernal, S.; Calvino, J. J.; Cauqui, M. A.; Perez-Omil, J. A.; Pintado, J. M.; Rodriguez-Izquierdo, J. M. *Appl. Catal. B Environ.* **1998**, *16*, 127.
(19) Colon, G.; Valdivieso, F.; Pijolat, M.; Baker, R. T.; Calvino, J. J.; Bernal, S. *Catal. Today* **1999**, *50*, 271.
(20) Fornasiero, P.; Kašpar, J.; Graziani, M. *J. Catal.* **1997**, *167*, 576.
(21) Bernal, S.; Calvino, J. J.; Cifredo, G. A.; Rodriguez-Izquierdo, J. M.; Perrichon, V.; Laachir, A. *J. Catal.* **1992**, *137*, 1.
(22) Hickey, N.; Fornasiero, P.; Kašpar, J.; Graziani, M.; Blanco, G.; Bernal, S. *Chem. Commun.* **2000**, 357.
(23) Anderson, J. R. *Structure of Metallic Catalysts*; Academic Press: London, 1975.
(24) Benson, J. E.; Hwang, H. S.; Boudart, M. *J. Catal.* **1973**, *30*, 146.
(25) Prelazzi, G.; Cerboni, M.; Leofanti, G. *J. Catal.* **1999**, *181*, 73.
(26) Ragaini, V.; Giannantonio, R.; Magni, P.; Lucarelli, L.; Leofanti, G. *J. Catal.* **1994**, *146*, 116.
(27) Conner, W. C., Jr.; Pajonk, G. M.; Teichner, S. J. Spillover of Sorbed Species. In *Advances in Catalysis*; Eley, D. D., Pines, H., Weisz, P. B., Eds.; Academic Press: Orlando, FL, 1986; vol. 34, pp 1−79.
(28) Di Monte, R.; Fornasiero, P.; Kašpar, J.; Rumori, P.; Gubitosa, G.; Graziani, M. *Appl. Catal., B, Environ.* **2000**, *24*, 157.
(29) Lafyatis, D. S.; Ansell, G. P.; Bennett, S. C.; Frost, J. C.; Millington, P. J.; Rajaram, R. R.; Walker, A. P.; Ballinger, T. H. *Appl. Catal., B, Environ.* **1998**, *18*, 123.
(30) Badri, A.; Binet, C.; Lavalley, J. C. *J. Chem. Soc., Faraday Trans.* **1996**, *92*, 1603.
(31) Chou, P.; Vannice, M. A. *J. Catal.* **1987**, *104*, 1.